

The permeability of clay suspensions

V. PANE* and R. L. SCHIFFMAN†

The chemical engineering literature abounds with empirical and theoretical equations relating the sedimentation and fluidization velocities of a given solid–liquid system and its porosity. A geotechnical approach shows that for active clay particles the problem lies in the definition, and associated determination, of a coefficient of permeability of the system. A fluidization test is proposed to provide a direct permeability measurement of clay suspensions. The experimental results obtained on two clay mixtures indicate that the coefficient of permeability varies continuously over a wide range of porosities, encompassing soil conditions and suspended conditions, and that a two-constant power equation can be usefully employed to represent such variation.

KEYWORDS: clays; laboratory tests; permeability; sedimentation.

Les textes de génie chimique abondent en équations empiriques et théoriques qui expérimentent les vitesses de sédimentation et de fluidisation d'un système solide–liquide donné et sa porosité. Une approche géotechnique montre que, pour des particules actives d'argile, le problème consiste à définir un coefficient de perméabilité du système et à le calculer. Les auteurs proposent un essai de fluidisation qui permet de mesurer directement la perméabilité d'argiles en suspension. Les résultats expérimentaux obtenus dans le cas de deux mélanges d'argile indiquent que le coefficient de perméabilité varie continuellement sur un vaste éventail de porosités, pour diverses conditions de sol et de suspension, et qu'on peut utiliser une équation à deux constantes pour représenter cette variation.

INTRODUCTION

Numerous disciplines are concerned with the relative motion which can be established between a fluid phase and a suspended solid phase. These disciplines include geotechnical engineering, sedimentology and chemical and environmental engineering, and the associated problems relate to sedimentation, consolidation, fluidization, erosion and mass transport.

Sedimentation has been used for industrial purposes since the early nineteenth century, and the study of the forces acting on a suspended solid goes back to Stokes, who in 1851 equated drag and gravitational forces to obtain the free-fall velocity of a single spherical particle in an infinite fluid:

$$v_{\text{Stokes}} = \frac{(\gamma_s - \gamma_w)d^2}{18\mu} \quad (1)$$

where d is the particle diameter, μ is the fluid viscosity and γ_s, γ_w are the unit weights of the solid and fluid phases respectively.

It is intuitive that, when the solid particle forms part of a suspension (i.e. when the porosity is less than unity), the relative flow established between the two phases must be influenced by the presence of the other particles, since they affect the flow pattern. In fact, with decreasing porosity the mutual interaction among the particles becomes so strong that particles of different size and shape may agglomerate and settle at the same rate. Under such conditions, particle segregation during settling is prevented and a sharp interface is formed between suspension and clear liquid above. This kind of settling is known as 'hindered' settling or 'zone' settling.

In spite of its practical importance, most of the experimental work on hindered settling prior to 1960 (Steinour, 1944; Hawksley, 1951; Loeffler & Ruth, 1959) was based on empirical and theoretical equations which related the settling velocity v_s of the suspension to Stokes's velocity of the single particle and to the system porosity n . For mixtures of inert particles, a fair fit with the experimental data was provided by a power function of the form

$$v_s = v_{\text{Stokes}} n^a \quad (2)$$

Manuscript received 18 June 1994; revised manuscript accepted 8 December 1995.

Discussion on this paper closes 1 September 1997; for further details see p. ii.

* University of Perugia.

† University of Colorado.

However, the exponent α in the above equation varied noticeably for the various mixtures investigated; for glass spheres, Lewis *et al.* (1949) found a constant value of α equal to 4.65. Richardson & Meikle (1961) carried out sedimentation tests with fine non-spherical particles of aluminium, 4–7 microns in average size, and showed that the value of α was greater than 10. Relaxing the assumption of equi-sized particles on the basis that no segregation occurs at high solid concentrations, McRoberts and Nixon (1976) observed the sedimentation of silty natural materials; the exponent α ranged from 5 to 30 in their experiments. In addition, most of these early studies implicitly assumed that the process is steady, so that v_s and n do not depend on time. A first departure from this traditional approach was furnished by Kynch (1952).

In the early 1940s another process involving a two-phase relative flow attracted the attention of chemical engineers; the technique of fluidizing solids with a gaseous flow was successfully applied to the catalytic cracking of petroleum fractions. Currently fluidization techniques are used for a variety of applications which include heat transfer, mass transfer and catalytic reactions.

The similarities between sedimentation and fluidization are outlined in Fig. 1. In a sedimentation process (Fig. 1(a)) a suspended solid phase moves downwards through a stationary fluid phase, under the action of gravity. On the other hand, in a fluidization process (Fig. 1(b)) a flow rate Q of a given fluid is forced upwards through a bed of solid particles. By gradually increasing the fluid

velocity, the particles tend to reorientate themselves until the loosest possible arrangement is achieved. When the fluid reaches a minimum 'fluidization velocity' v_f , the particles are kept in suspension by the upward flow—that is, the bed is fluidized. In such stationary conditions, the bed remains at a constant porosity, and the solid particles retain their mean position with time ($v_s = 0$). This type of fluidization is known as 'particulate' (Kunii & Levenspiel, 1969) since the solid phase remains evenly dispersed in the fluid and a sharp stationary interface is maintained between the suspension and the clear liquid above.

The early experimental findings on fluidization (Brinkman, 1947; Verschoor, 1950; Hanratty & Bandukwala, 1957) soon revealed that the fluidization and sedimentation velocities of a given system at a given porosity were practically coincident. A rational explanation of this behaviour was given by Richardson & Zaki (1954), whose rigorous hydrodynamics analysis furnished the theoretical understanding of the two-phase vertical flow and revealed the observed similarities between sedimentation and fluidization processes. Such analysis may be summarized by two fundamental statements of chemical engineering.

- (a) The fluidization velocity necessary to maintain a uniform system at a given porosity is equal (and opposite) to the settling velocity of the same system at the same porosity.
- (b) For a given solid–fluid system, the velocity of fluidization and the velocity of sedimentation depend only on the system porosity:

$$v_s = -v_f = v_{\text{Stokes}} f(n) \quad (3)$$

Equation (3) holds for inert spherical particles when either skin friction (laminar flow) or form drag (turbulent flow) is predominant.

THE PERMEABILITY OF SUSPENSIONS

We now show that a geotechnical approach to the problem leads, in a rather straightforward manner, to the same conclusions as given above, and to the definition of a coefficient of permeability for suspended conditions. Figs 1(a) and (b) show respectively a sedimentation and a fluidization test conducted on two identical mixtures at the same porosity. Let

$$v_f = nv_w = Q_f/A \quad (4)$$

be the fluidization velocity for the test shown in Fig. 1(b), referred to the empty area of the column A . Since the mean velocity of any particle equals zero, the relative velocity ($v_s - v_w$) between the two phases is

$$\text{fluidization: } v_s - v_w = -v_f/n \quad (5)$$

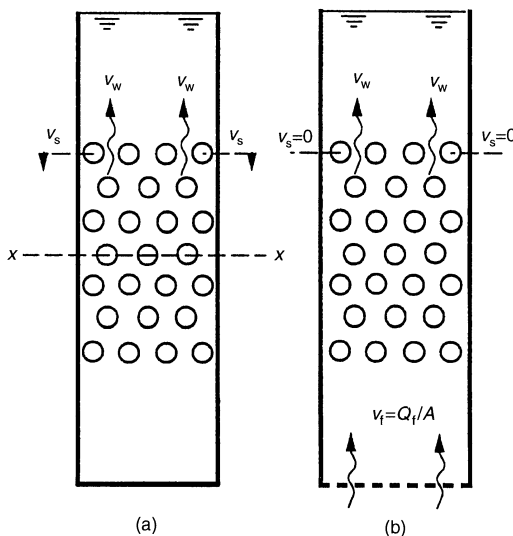


Fig. 1. Sedimentation and fluidization processes: (a) sedimentation; (b) fluidization

On the other hand, for the sedimentation test in Fig. 1(a), assuming that both solid particles and fluid are incompressible, continuity requires that the volume of matter below any horizontal section $x-x$ is constant, that is

$$(1 - n)v_s + nv_w = 0 \quad (6)$$

From the above equation, the relative velocity between the two phases during sedimentation is found to be

$$\text{sedimentation: } v_s - v_w = v_s/n \quad (7)$$

Furthermore, since the solid particles in Fig. 1 are entirely supported by the fluid, the total vertical stress σ is equal to the total pore pressure, or

$$\sigma = u_0 + u \quad (8)$$

where u is the excess pore pressure over the hydrostatic pressure u_0 . The vertical equilibrium of the mixture may be expressed by differentiating equation (8) with respect to the Eulerian coordinate x , directed with gravity. This leads to

$$\frac{\partial u}{\partial x} = (\gamma_s - \gamma_w)(1 - n) = \gamma' \quad (9)$$

where γ' is the buoyant unit weight of the mixture.

We now invoke an experimental principle attributed to Gersevanov (1934), representing a generalization of Darcy's law:

$$n(v_s - v_w) = \frac{k(n) \partial u}{\gamma_w \partial x} \quad (10)$$

where the coefficient of permeability of the mixture k is assumed to depend uniquely on mixture porosity. The introduction of the relative velocity in the above equation extends Darcy's law to a variety of processes involving relative flow between two phases. In fact, by substituting the Darcy-Gersevanov equation (10) into equations (5) and (7), and taking account of equation (9), one finds

$$v_s = -v_f = \gamma^*(1 - n)k(n) = \gamma^* \frac{k(e)}{(1 + e)} \quad (11)$$

where e is the void ratio and the non-dimensional constant γ^* is given by

$$\gamma^* = (\gamma_s - \gamma_w)/\gamma_w \quad (12)$$

Equation (11) is formally identical to the one

obtained by Richardson and Zaki (equation (3)). This provides a theoretical background to the experimental principle invoked, and furnishes a definition for the permeability of suspensions.

THE EXPERIMENTAL DETERMINATION OF k

Equation (11) suggests two independent testing approaches to provide a direct permeability measurement on a suspension, which are

(a) a steady-state fluidization test on a uniform dispersion of void ratio e , and the determination of k from the fluidization velocity according to

$$k(e) = \frac{v_f(1 + e)}{\gamma^*} \quad (13)$$

(b) a transient sedimentation test on a uniform dispersion of void ratio e , and the determination of k from the initial settling velocity of the suspension according to

$$k(e) = \frac{v_{si}(1 + e)}{\gamma^*} \quad (14)$$

where v_{si} is the initial settling velocity of the solids.

Both of the above approaches have been used in this work. It is noted that an equation formally identical to equation (14) above has been derived by Been (1980); however, due to the propagation of continuity and discontinuity waves originating from the bottom of the sedimenting column (Kynch, 1952), the equation is valid only as long as there is suspension of the initial porosity at the sediment-water interface, that is, as long as the surface settling velocity is constant.

Materials and experimental procedure

In order to obtain conditions of 'hindered settling' in the sedimentation tests and of 'particulate fluidization' in the fluidization tests, particle segregation and differential settling of the mixture had to be minimized. Hence a rather inert artificial clay, such as Speswhite kaolin, was chosen for the initial stage of the investigation. The index properties of the kaolin (a commercially available powder provided by Whitfield and Sons, UK) are summarized in Table 1.

Table 1. Index properties of Speswhite kaolin and phosphatic clay

	Specific gravity: G_s	Clay fraction: %	Liquid limit w_L : %	Plastic limit w_p : %	Activity	Main clay minerals
Speswhite kaolin	2.60	75	53	32	0.28	Kaolinite
Phosphatic clay	2.74	70	162	44	1.67	Smectite, attapulgite, illite

Particle aggregates relatively uniform in size were obtained by means of flocculation and standardized mixing procedures. Sodium chlorite at a relatively high concentration (23 g/l) was chosen as a flocculating agent. Under such conditions, the kaolin is flocculated in a 'card-pack' form with a predominant face-to-face orientation (Michaels, 1958). It has been shown that the mixing procedure has a substantial effect on the settling behaviour of suspensions, and that the shear field in the suspension determines the shape and the dimensions of the flocs and of their aggregates (Bolger, 1960). In particular, moderate mixing intensities, such as those obtained by inverting the suspension, produce smaller aggregates within a relatively narrow size range. A mild-agitation mixing procedure was then adopted to prepare the kaolin suspensions for all sedimentation and fluidization tests. The dry powder was weighed, mixed with the pore fluid at the desired initial porosity, blended for

5 min into a high-speed Waring blender and then allowed to settle overnight in a 1000 ml jar. At the start of the tests, the jar was inverted 20 times and the suspension was poured into either a sedimentation cylinder or the fluidization column described below. All tests were performed at a constant temperature of $22 \pm 0.5^\circ\text{C}$. To determine the initial porosity of the mixture, hydrometer readings were taken prior to the tests for both the suspensions and a batch of the pore fluid at the same temperature, the latter serving as a reference. The hydrometer measurements were repeated until three consecutive readings within 2% of the measured density were obtained. The mixture was inverted after each hydrometer measurement.

In order to check the test repeatability, a series of six duplicate tests was performed at different values of the initial void ratio e_0 . These are grouped in Fig. 2, showing the progress of settlement of the sharp interface formed between

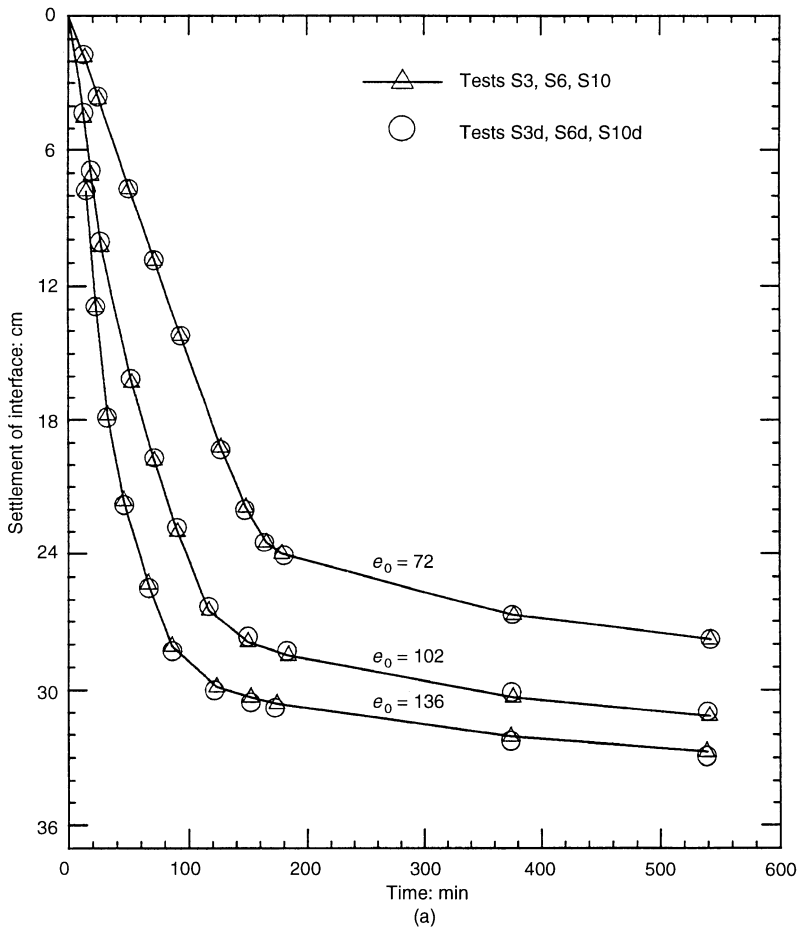


Fig. 2. Duplicate settling tests on Speswhite kaolin

suspension and clear liquid above (the letter 'd' denotes duplicate tests). From these figures it is noted that the above-mentioned procedure resulted in an excellent reproducibility, with both settling rates and final sediment heights being very close for the duplicate tests.

Sedimentation tests

With the mixing procedure adopted it was found that hindered settling conditions, characterized by a smooth, well-defined upper interface, could be achieved for void ratios ranging between approximately 40 and 140. For higher porosities, the interface appeared slightly blurred and undefined, indicating some particle segregation. On the other hand, for lower porosities channelling was observed and some surface features of the interface (such as miniature craters and volcanoes) indicated a very small but finite shear strength, and thus the

initiation of effective stresses. Table 2 summarizes the series of 10 sedimentation tests performed on uniform suspensions at initial void ratios ranging between 40 and 136. Most of the tests were performed in standard sedimentation glass cylinders

Table 2. Summary of sedimentation tests on Speswhite kaolin

Test	e_0	h_0 : cm	h_z : cm	h_s : cm	e_s
S1	40	34.7	0.846	18.3	20.6
S2	60	37.6	0.616	15.2	23.7
S3	72	37.0	0.507	13.0	24.6
S4	82	37.3	0.452	11.8	25.1
S5	90	36.3	0.399	10.5	25.3
S6	102	37.0	0.359	9.4	25.2
S7	123	40.0	0.323	9.2	27.5
S10	136	37.0	0.270	7.7	27.5
S8	123	29.6	0.239	6.9	27.9
S9	123	17.6	0.142	4.2	28.5

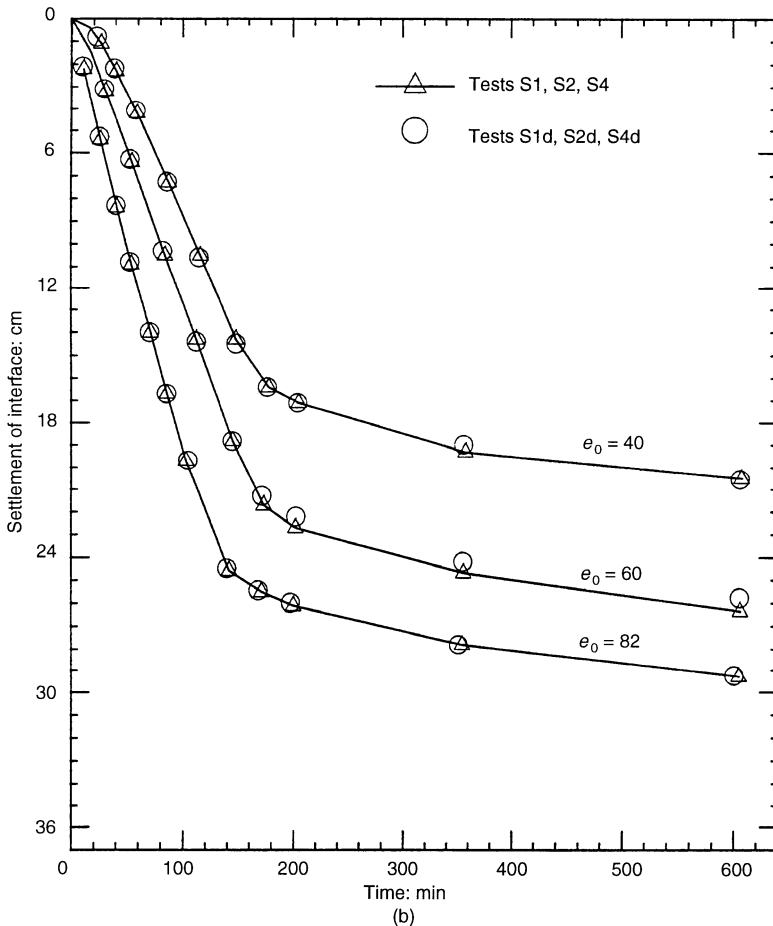


Fig. 2(cont.). Duplicate settling tests on Speswhite kaolin

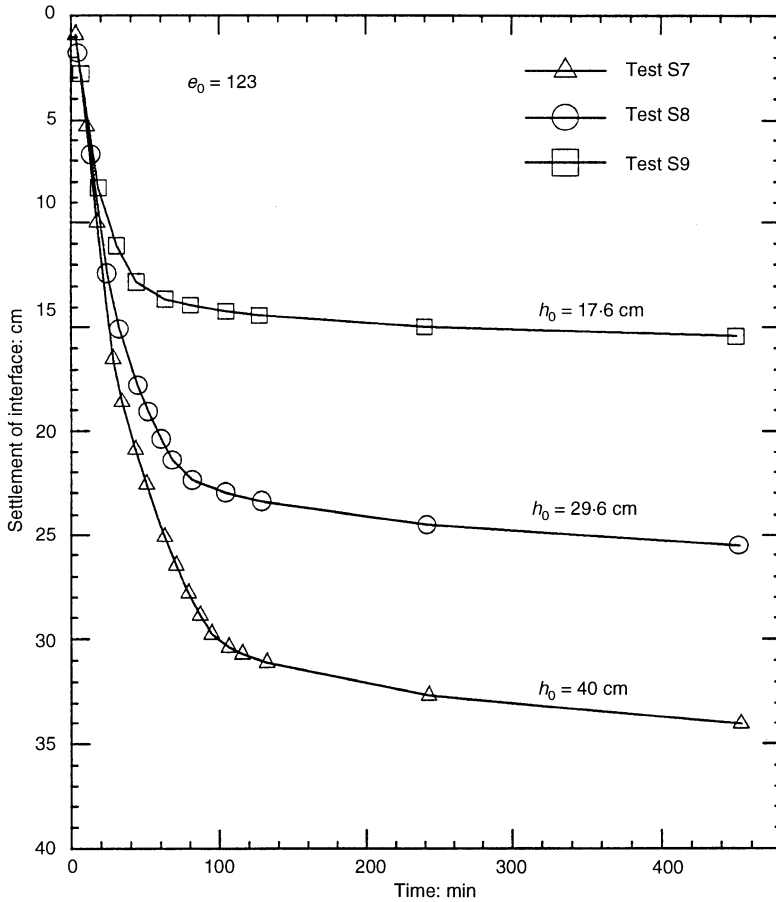


Fig. 3. Settling tests on Speswhite kaolin using different initial heights

(6.3 cm internal diameter), the initial height of the suspension h_0 varying between 34 and 38 cm. Visual observations allowed one to detect the position of the upper interface with an accuracy of 0.5 mm. Tests S7, S8 and S9, shown in Fig. 3, had the same initial void ratio ($e_0 = 123$) but markedly different initial heights; also, in this case the uniqueness of the initial settling velocity of the interface was noted.

Some general observations on the process of soil formation can be drawn with reference to Fig. 4, where a typical test is depicted. The figure shows that the sedimentation and consolidation regions are separated by a soil formation line (0A) characterized by a constant value of the void ratio e_m , herein denoted as 'soil-formation void ratio'. At a time t_s of the order of 180 min, when the thickness of the accumulated sediment h_s is about 13 cm, the soil formation line intersects the upper interface of the suspension and the settling velocity

abruptly decreases, indicating the completion of the sedimentation stage. Although the soil formation line was not apparently visible for any of the tests performed, the line 0A in Fig. 4 is qualitatively drawn with a slight downward concavity to indicate that the accumulated soil is undergoing a self-weight consolidation process while accreting; most of the consolidation, however, occurs after completion of the sedimentation stage, the time to achieve full consolidation being two order of magnitudes larger than t_s .

A lower limit to e_m for the Speswhite kaolin can be inferred by considering that the total thickness of the solid matter h_z (i.e. the material height) for each of the settling tests is constant throughout the sedimentation/consolidation process, that is

$$h_z = \frac{h_0}{1 + e_0} = \frac{h_s}{1 + e_s} = \text{constant} \quad (15)$$

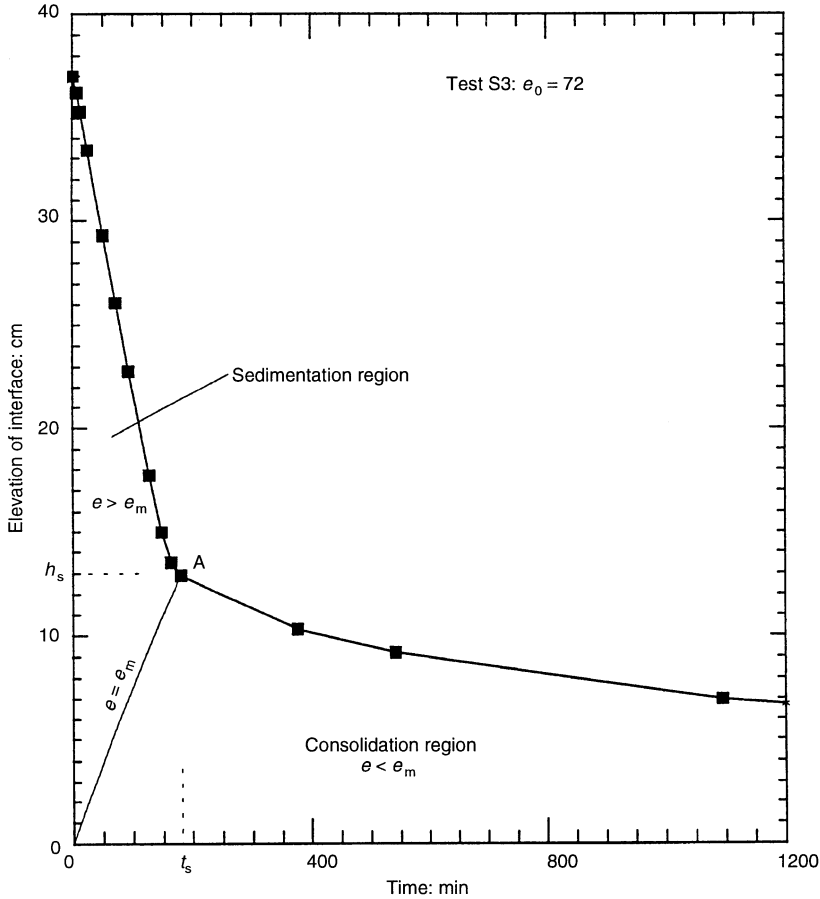


Fig. 4. Process of soil formation

where e_s is the average void ratio in the accumulated sediment at time t_s . Hence the value of e_m must satisfy the following relationship:

$$e_m \geq e_s = \frac{h_s}{h_z} - 1 \tag{16}$$

in which the difference between e_m and e_s increases with increasing consolidation in the sediment at time t_s . Table 2 summarizes the estimated values of h_s and e_s for the full set of settling tests, listed in order of decreasing material height. It is noted that the calculated values of e_s monotonically decrease with increasing material height h_z , which indicates some consolidation occurring below the soil formation line during the sedimentation stage, but they are relatively close to each other when compared with the wide range of initial void ratios. From the listed values, it seems reasonable to state that the soil-formation void ratio of the Speswhite kaolin is slightly greater than 28 and relatively independent of the initial porosity of the suspension. A further

confirmation of these findings is furnished by the inversion process of the coupled theory of sedimentation and consolidation, briefly mentioned below, which yields

$$e_m = \text{constant} = 30 \tag{17}$$

Hence e_m may be regarded as a fundamental material property of a given clay-water mixture, for a given set of chemical and environmental conditions.

In order to determine the permeability of the suspensions, only the early stages of settling are of interest; these are reported in Fig. 5 for the various porosities investigated. From Fig. 5 it is apparent that there is a relatively short flocculation period characterized by a smaller velocity of the interface. On completion of the flocculation stage, however, the settling velocity of the interface approaches a fairly constant value v_{st} . An exception is noted for test S1 at the lowest void ratio ($e_0 = 40$), in which channels as large as 0.5 mm in diameter immedi-

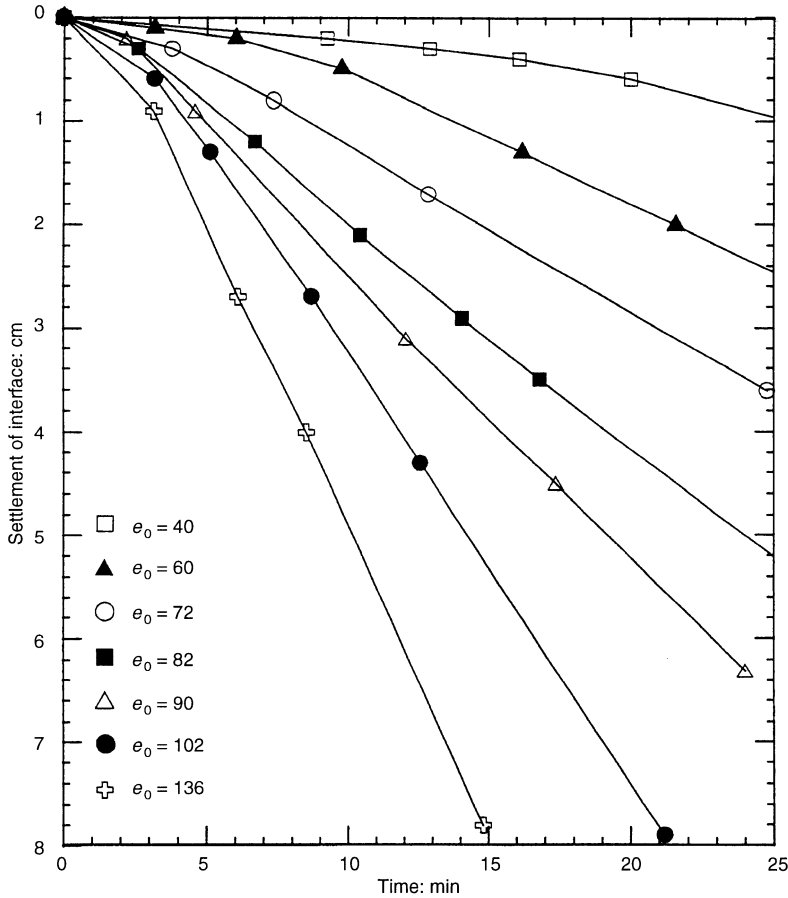


Fig. 5. Early stages of sedimentation tests on Speswhite kaolin

ately appeared in the bottom of the suspension, elongated upwards during the sedimentation stage and finally disappeared at the end of this stage. As a direct consequence of this preferential upward flow, the velocity of the interface steadily increased until the completion of the sedimentation stage.

Values of v_{si} and the corresponding values of k , calculated from equation (14), are reported in Table 3 for the different mixture porosities; the ranges shown correspond to the ranges in the values of v_{si} observed in the settling plots of Figs 2-4.

Table 3. Values of k from sedimentation tests on Speswhite kaolin

Test	e_0	n_0	Range of v_{si} : 10^{-5} m/s	Range of K : m/s
S1	40	0.976	0.6-2.0	$1.5-5.0 \times 10^{-4}$
S2	60	0.984	1.5-2.3	$5.7-8.7 \times 10^{-4}$
S3	72	0.986	2.7	1.2×10^{-3}
S4	82	0.988	3.8	2.0×10^{-3}
S5	90	0.989	4.0	2.3×10^{-3}
S6	102	0.990	6.7	4.4×10^{-3}
S7, S8, S9	123	0.992	8.8-9.2	$6.9-7.1 \times 10^{-3}$
S10	136	0.993	9.7-10.0	$8.3-9.0 \times 10^{-3}$

Fluidization tests

Steady-state fluidization tests were performed by means of the experimental apparatus schematically shown in Fig. 6, according to the following steps. A uniform soil-water mixture of void ratio e , prepared according to the above procedure, is poured into the fluidization column. Then an upward flow

rate Q_f of the same pore fluid is forced into the suspension through the distributor at the bottom of the column, until the interface between suspension and supernatant liquid is stationary. The measurement of Q_f and of the corresponding fluidization

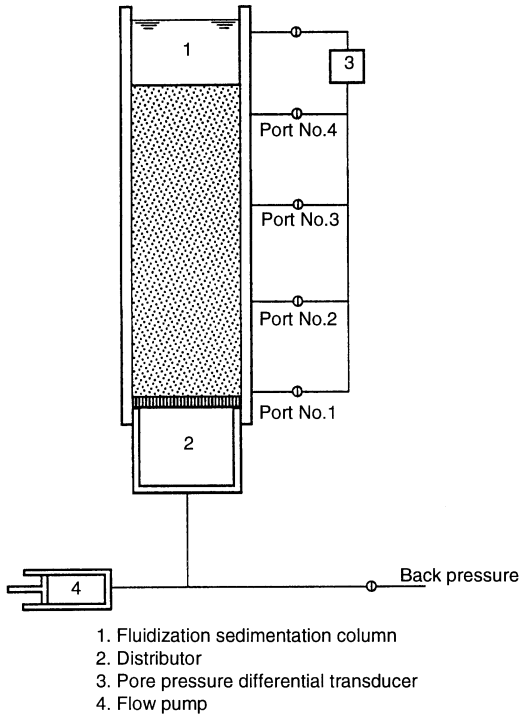


Fig. 6. Schematic layout of experimental apparatus

velocity ($v_f = Q_f/A$) provides the value of k from equation (13). Theoretically, several values of $(k(e), e)$ may be obtained in one prolonged test in which the flow rate is monotonically increased in small steps and then kept constant, until steady state is achieved at a higher void ratio.

The fluidization column consisted of a graduated acrylic tube, 80 cm high and 6.3 cm internal diameter. An imperative requirement for the achievement of particulate fluidization is to ensure a uniform flow of the pore fluid at the bottom of the suspension. This is accomplished by a properly designed distributor. Early experiments (Grohse, 1955; Takeda, 1957; Zenz & Othmer, 1960) have shown that the quality of particulate fluidization is strongly influenced by the type of distributor used, and that the tendency for channelling and non-uniformity in local porosities is minimized by using sintered porous plates. In addition, the distributor should provide a sufficient pressure drop to achieve equal flow through the openings (Kunii & Levenspiel, 1969). These considerations led to the design of the distributor shown in Fig. 7, which includes:

(a) Two sintered metal porous plates (provided by Mott Metallurgical Corporation) with an average pore size of $5 \mu\text{m}$, that is, smaller than the

likely floc dimensions. The outer portions of the plates were machined and coated in order to provide leak-free seals between the plates and the upper and lower O-rings (Nos. 1 and 2 in Fig. 7). The machined portion of the plates was contained within the thickness of the acrylic tube to ensure uniform flow near the walls of the tube.

(b) A bed of fine sand packed between two screens of stainless steel, and a calming section above it to reduce turbulence effects and agitation of the fluid entering the porous plates.

The upward constant flow was provided by a flow pump-syringe system similar to the one used to perform permeability tests on soils (Olsen, 1966; Aiban & Znidarcic, 1989). By means of an electronically variable DC motor, the velocity of the flow pump (Model 906, Harvard Precision Pumps) could be varied in a continuous fashion, producing an overall motor speed range of 110 000 to 1 with reproducibility and accuracy better than $\pm 1.5\%$ and $\pm 5\%$ respectively.

Excess pore pressures could be measured at four fixed elevations along the column by means of a differential pressure transducer (Valadine DP103 Ultra Low Range). The upper port, being always immersed in the supernatant clear fluid, served as a reference for the other four measurements. The transducer had interchangeable diaphragms for different pressure ranges. The most sensitive diaphragm, in particular, revealed excellent sensitivity (5×10^{-4} kPa) and fair accuracy ($\pm 5 \times 10^{-3}$ kPa), but high flexibility. The latter, however, did not seem to represent a major inconvenience for the performance of fluidization tests owing to the steady-state nature of these tests and the high permeability of the mixtures.

Six fluidization tests were performed on uniform suspensions of Speswhite kaolin within the range of void ratios pertinent to hindered settling conditions. As an example, the raw data relative to one of the tests (test F5, $e_0 = 95$) are reported in Table 4; the stability of the interface and of the pore pressure readings at the four ports during the 17 min test indicates the achievement of steady-state conditions. It is parenthetically noted that in the absence of the upward flow rate, the settlement δ of the suspension during the 17 min test would have been approximately equal to:

$$\delta \approx v_s t = v_f t = 51-55 \text{ mm} \quad (18)$$

Since the interface was kept within 1 mm of its original position with a fluidization velocity lying in the narrow range $5.0-5.4 \times 10^{-5}$ m/s, the approximation in the measured value of k is of the order of 10% for this particular test.

Qualitatively similar conclusions about the test approximation can be drawn for the other fluidiza-

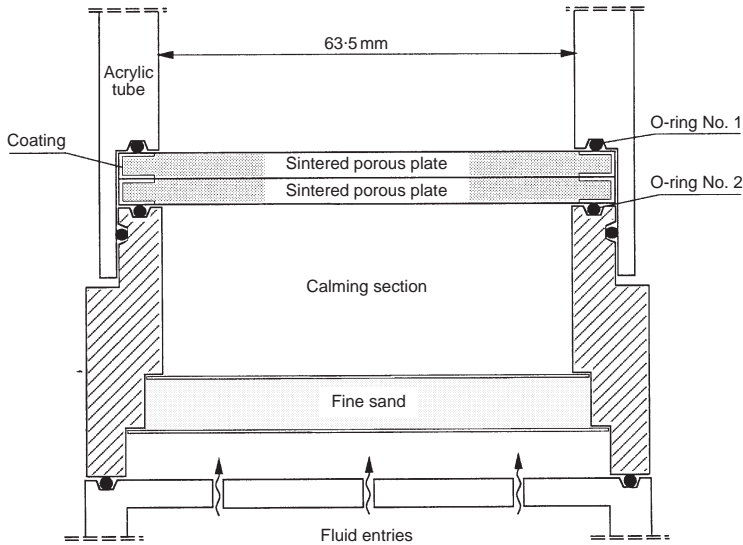


Fig. 7. Detail of the distributor

Table 4. Fluidization test F5 ($e_0 = 95$): measured values of v_B and u

Time: min	Elevation of interface:	v_f : 10^{-5} m/s	Excess pore pressure u : kPa			
			Port No. 1	Port No. 2	Port No. 3	Port No. 4
0	36.1	5.4	0.061	—	—	—
2.0	36.1	5.4	0.061	—	—	—
2.7	36.1	5.4	—	0.048	0.037	0.024
5.0	36.1	5.4	—	—	—	—
7.5	36.2	5.3	0.061	0.048	0.037	0.024
9.5	36.2	5.2	—	—	—	—
13	36.2	5.0	0.061	0.048	0.036	0.024
17	36.2	5.0	0.061	0.048	0.036	0.024

tion tests, summarized in Table 5, where the ranges in the values of k correspond to the ranges of fluidization velocities imposed during the test to keep a stationary interface. An exception is noted

for test F1 at the lowest void ratio ($e_0 = 35$), during which channelling was observed and the value of v_f had to be monotonically and significantly increased in order to maintain a stationary

Table 5. Values of k from fluidization tests on Speswhite kaolin

Test	e_0	n_0	Test duration: min	Range of v_f : 10^{-5} m/s	Range of k : m/s	Pore pressure measurements
F1	35	0.972	78	0.6–1.7	$1.4-3.8 \times 10^{-4}$	Yes
F2	54	0.982	48	1.7–2.0	$4.9-6.9 \times 10^{-4}$	Yes
F3	72	0.986	17	2.5–2.7	$1.1-1.2 \times 10^{-3}$	Yes
F4	87	0.989	16	4.2–4.5	$2.3-2.5 \times 10^{-3}$	No
F5	95	0.990	17	5.0–5.4	$3.0-3.2 \times 10^{-3}$	Yes
F6	129	0.992	9	9.2–9.7	$7.5-7.9 \times 10^{-3}$	No

interface. This behaviour is analogous to the one exhibited during sedimentation, at comparable values of the void ratios (test S1, $e_0 = 40$).

It is emphasized that the fluidization test does not require the measurement of a head drop. In fact equation (9) shows that for dispersed conditions the excess pore pressure gradient *must* be equal to the buoyant unit weight of the mixture, and hence its measurement is redundant. Nevertheless, pore pressure measurements taken at several locations can be extremely useful to prove the validity of equation (9) and to assess the uniformity of the suspension during the test, that is, the test quality. For this purpose, four of the fluidization tests listed in Table 5 were performed with measurements of the excess pore pressure, u . A comparison between the measured and theoretical values of u , shown in Fig. 8, reveals that

- (a) the total pore pressure is indeed equal to the total vertical stress throughout the fluidized column
- (b) the excess pore pressure gradient is sensibly

constant along the column—that is, the suspension is actually fluidized at a uniform void ratio.

EXPERIMENTAL RESULTS

The values of k obtained for the suspensions of Speswhite kaolin by means of the above sedimentation and fluidization tests are shown in Fig. 9, in the usual semi-logarithmic plot against the void ratio.

The figure also shows the values of k of the kaolin in soil conditions ($1 < e < 3.5$), obtained by flow pump permeability tests performed at gradients lower than 5. In this case the specimens were prepared by mixing the dry powder with distilled water at a water content equal to 2.5 times the liquid limit, and then poured into Anteus (Model A-1) back-pressurized oedometers. Step-loading tests were then performed with permeability measurements made at the end of each load increment (Pane *et al.*, 1983).

The continuous line joining the experimental

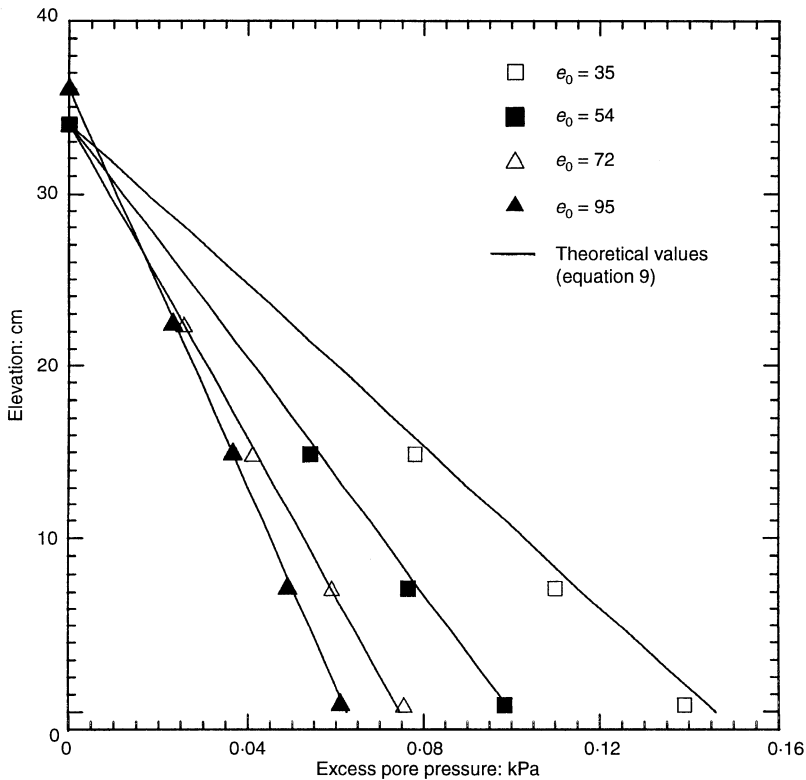


Fig. 8. Measured and theoretical excess pore pressures for fluidization tests on Speswhite kaolin

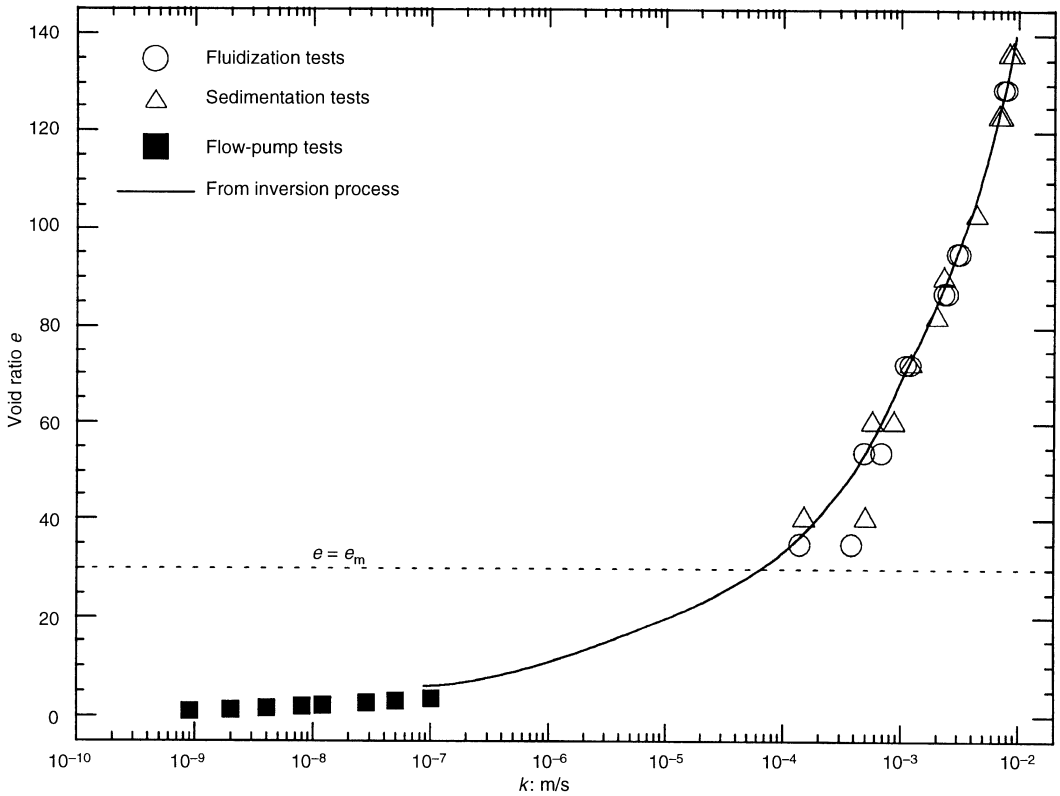


Fig. 9. Void ratio–permeability relationship of Speswhite kaolin

data points is obtained from an inversion process of the theory of coupled sedimentation and consolidation (Pane, 1985; Pane & Schiffman, 1985). In such an inversion procedure, the parameters of the theory (namely, the soil-formation void ratio e_m , the void ratio–effective stress relationship and the void ratio–permeability relationship) are adjusted with a trial and error procedure to optimize the fit between measured and predicted settlements during the sedimentation and consolidation stages of the settling test. This aspect of the problem goes beyond the purpose of the present work and will be treated in a subsequent paper.

The horizontal dotted line shown in Fig. 9 corresponds to the soil formation void ratio ($e_m = 30$), dividing dispersed conditions from soil conditions for the mixture at hand.

The following inferences can be drawn from the data presented in Fig. 9.

(a) The values of k measured from fluidization and sedimentation tests for the dispersed state

($e > e_m$) are practically coincident, confirming the validity of equation (11).

- (b) The relatively large ranges in the values of v_{si} , v_f and k obtained from both fluidization and sedimentation tests for the mixtures at the lowest void ratios (test F1, $e_0 = 35$; test S1, $e_0 = 40$) clearly indicate that at these porosities effective stresses start to manifest themselves and hindered settling conditions are no longer possible. For such values of the void ratios, which are close to the soil-formation void ratio, the mixture exhibits channelling and other fabric changes—that is, what has been defined by previous workers as a transitional or ‘intermediate’ behaviour between suspensions and soils (Michaels & Bolger, 1962; Been & Sills, 1981).
- (c) There appears to be continuity between the values of k in suspended conditions and soil conditions.
- (d) The variation of permeability is enormous; the values of k increase seven orders of magnitude for void ratio changes of about two orders of

magnitude, and at the highest values of the void ratio considered here ($e \approx 140$) the permeability of the kaolin mixture approaches that of a clean coarse sand ($k \approx 10^{-2}$ m/s).

- (e) There exists a range of void ratio below e_m (say, $5 < e < 30$) in which the direct determination of k by means of available experimental techniques encounters serious difficulties; among these, the highly non-uniform distribution of the void ratio within the sample due to its self-weight, and the necessity of imposing extremely low gradients to minimize the effects of seepage-induced consolidation. It is likely that in such a range the coefficient of permeability must be estimated indirectly, that is, from an inversion procedure of a consolidation process.

An observation may be drawn regarding the variation of k with the void ratio under conditions of extreme dilution. By taking the limit of equation (11) when the solid concentration tends to zero, it is found that

$$\lim_{e \rightarrow \infty} \gamma^* \frac{k}{(1 + e)} = \lim_{e \rightarrow \infty} v_s(e) = v_{Stokes} \quad (19)$$

This implies that for extremely diluted suspensions the term $\gamma^*k/(1 + e)$ tends to the Stokes velocity of a single aggregate, and hence that k varies linearly with e . The values of $\gamma^*k/(1 + e)$ corresponding to the k values of Fig. 9 are plotted as a function of e in Fig. 10; even at the highest void ratios considered here, the values of $\gamma^*k/(1 + e)$ are far from reaching a horizontal asymptote. This suggests that the solid concentrations used in this study are well within the range of hindered settling, and that the free-fall velocity of a single floc of the mixture at hand is sensibly larger than the ones reported here.

It is noted that the relationship between $\log k$ and e shown in Fig. 9 is highly non-linear. However, if the same experimental data are reported in the bi-logarithmic plot of Fig. 11 a sensibly linear regression is obtained. Fig. 11 also shows the values of permeability data measured by means of constant rate of strain ($4 < e < 18$) and sedimentation tests ($120 < e < 380$) on a second, more active clay-water mixture, a phosphatic clay. The clay, which is the waste product of phosphate mining operations in Florida (Carrier & Beckman, 1984), contains significant fractions of active clay minerals as indicated by the index properties

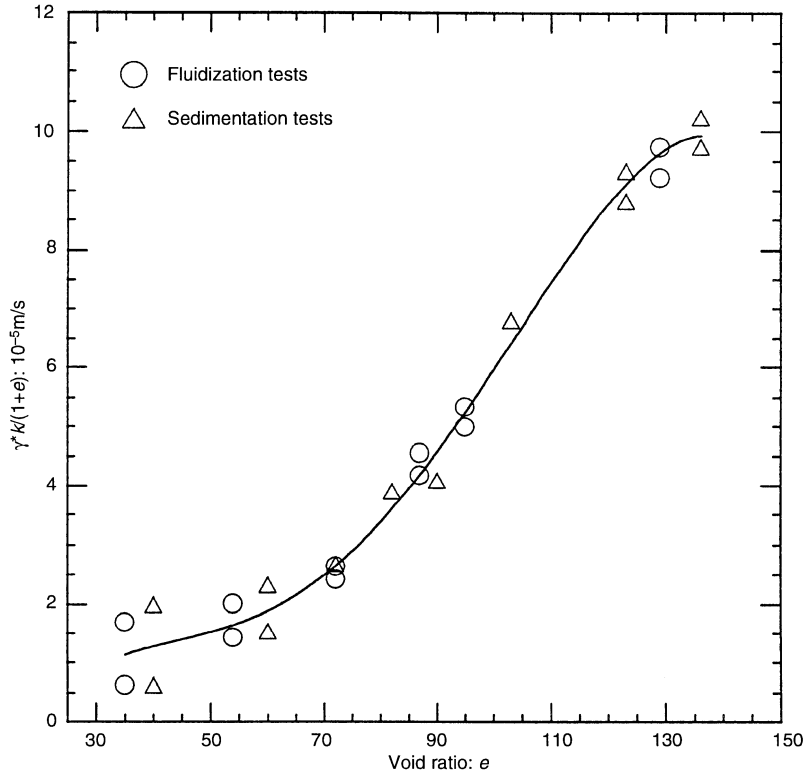


Fig. 10. Void ratio plotted against $\gamma^*k/(1 + e)$ for Speswhite kaolin

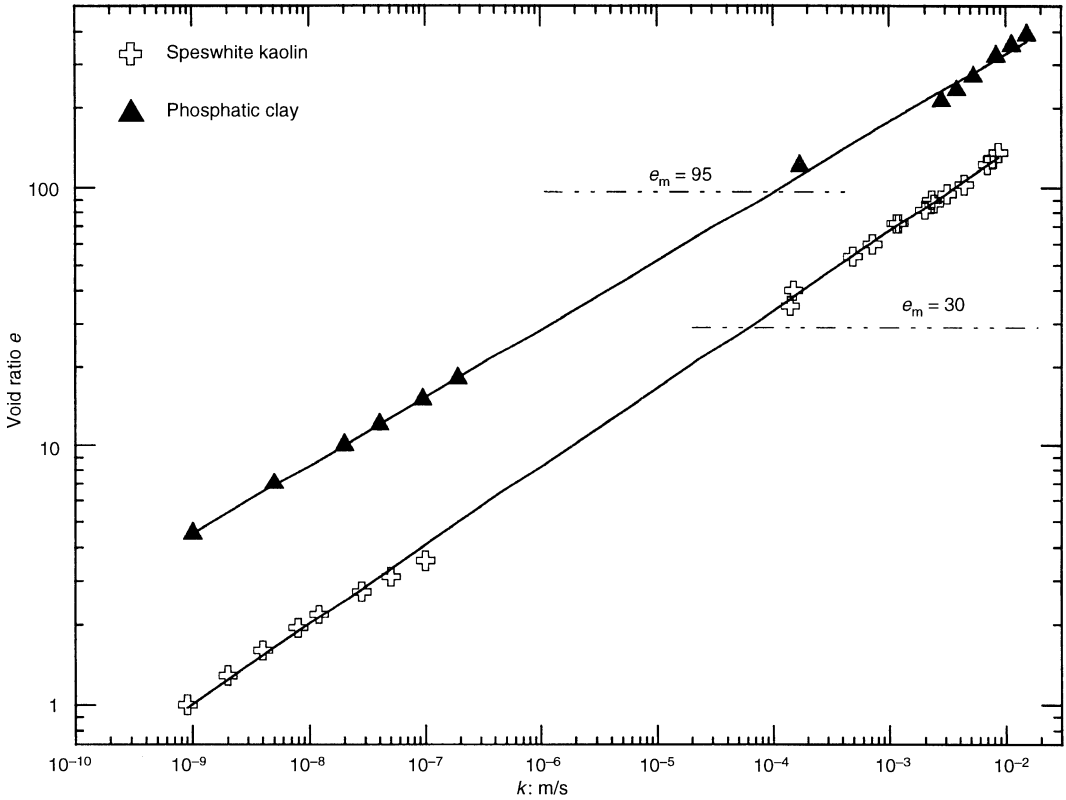


Fig. 11. Void ratio–permeability relationships of Speswhite kaolin and phosphatic clay

summarized in Table 1. This is also reflected in the extremely high value of the soil-formation void ratio pertinent to such material ($e_m = 95$). As expected, the permeability of the phosphatic clay is sensibly lower than the one of the Speswhite kaolin, at comparable void ratios.

The experimental data presented in Fig. 11 indicate that a power equation of the form

$$k = Ce^D \tag{20}$$

can be employed to describe the variation of k with the void ratio. Table 6 summarizes the values

of the constants C and D for the two mixtures under investigation, together with the coefficients of determination, r^2 , obtained from the power fits of Fig. 11. The slightly different values of C and D relevant to the Speswhite kaolin in soil conditions ($1 < e < 3.5$) and suspended conditions ($35 < e < 136$) could be attributed to the different mixing procedures and pore fluid employed for the specimen preparation, which are likely to result in different microstructures. However, the difference seems to be overwhelmed by the enormous range of void ratio, so that a single power relationship

Table 6. Power fits of void ratio–permeability data

Mixture	D	C : m/s	r^2
Speswhite kaolin			
Suspension ($35 < e < 136$)	3.21	1.3×10^{-9}	0.995
Soil ($1 < e < 3.5$)	3.67	7.7×10^{-10}	0.994
Whole range	3.28	1.0×10^{-9}	0.999
Phosphatic clay			
Suspension ($120 < e < 380$)	3.75	3.7×10^{-12}	0.969
Soil ($4 < e < 18$)	3.80	3.2×10^{-12}	1.000
Whole range	3.76	3.5×10^{-12}	0.999

provides a fair interpolation across the whole range of experimental data points.

It is noted that power equations similar to equation (20) have been suggested in the past by several investigators in dealing with soft soils (Carrier & Beckman, 1984; Krizek & Somogyi, 1984; Al Tabbaa & Wood, 1987). The present work shows that such a relationship may be usefully employed to cover the whole range of porosities normally encountered for consolidation and hindered settling processes.

CONCLUSIONS

This study shows that, by employing a generalized form of Darcy's law, the definition of permeability of porous media can be extended to cover soil-water mixtures in suspended conditions. The flow equation so obtained,

$$v_s = -v_f = \gamma^* k(n)(1-n) = \gamma^* \frac{k(e)}{(1+e)} \quad (11)$$

is formally identical to the one which has been extensively observed, and theoretically found, for the sedimentation, thickening and fluidization processes encountered in several natural and artificial situations.

A new permeability test, the fluidization test, is proposed to infer a permeability measurement for suspensions of clay particles. This test does not require the measurement of a head drop. Alternatively, the permeability of the suspensions may be estimated from the settling velocity recorded in the early stage of a sedimentation test.

The results obtained on two clay mixtures of different activity show that the variation of k is smooth and continuous over a wide range of mixture porosity, extending from soil conditions ($n = 0.5$) to suspended conditions ($n = 0.99$), and that a two-constant power equation (equation (20)) can be usefully adopted to represent the variation of k in such range of porosities.

The value of the soil-formation void ratio e_m , although depending on the mineral and fluid composition, does not seem to be influenced by the initial porosity of the suspension.

This work has shown the continuity of the coefficient of permeability during the process of sedimentation and consolidation. We leave to a subsequent paper the mathematical description of this coupled process, and its corroboration by means of experimental results.

ACKNOWLEDGEMENT

We are pleased to acknowledge the financial support provided by the US National Science Foundation. We are also indebted to the referees for their valuable and helpful comments.

NOTATION

A	area of empty column
C, D	constants in equation (20)
d	particle diameter
e	void ratio
e_m	soil-formation void ratio
e_0	initial void ratio of the laboratory mixtures
f	generic function in equation (3)
h_0	initial height of the suspension
h_s	thickness of accumulated soil at the end of the sedimentation stage
h_z	material height of the suspension
k	coefficient of permeability
n	porosity
n_0	initial porosity of the laboratory mixtures
Q	flow rate
Q_f	fluidization flow rate
r^2	coefficient of determination of power fits to equation (20)
t	time
t_s	time at the end of the sedimentation stage
u	excess pore pressure
u_0	hydrostatic pore pressure
v_f	fluidization velocity
v_s	velocity of the solids
v_{si}	initial settling velocity of the solids in a sedimentation test
v_{Stokes}	Stokes's free-fall velocity of a spherical particle
v_w	velocity of the fluid
x	Eulerian coordinate (positive with gravity)
α	exponent in equation (2)
δ	settlement of the suspension
γ_s	unit weight of the solid particles
γ_w	unit weight of the fluid
γ'	buoyant unit weight of the mixture
γ^*	non-dimensional constant in equation (12)
μ	fluid viscosity
σ	total vertical stress

REFERENCES

- Aiban, S. A. & Znidarcic, D. (1989). Evaluation of the flow pump and constant head techniques for permeability measurements. *Géotechnique* **39**, No. 4, 655–666.
- Al Tabbaa, A. & Wood, D. W. (1987). Some measurements of the permeability of kaolin. *Géotechnique* **37**, No. 4, 499–503.
- Been, K. (1980). *Stress strain behaviour of a cohesive soil deposited under water*. University of Oxford, PhD thesis.
- Been, K. & Sills, G. C. (1981). Self-weight consolidation of soft soils: an experimental and theoretical study. *Géotechnique* **31**, No. 4, 519–535.
- Bolger (1960) *Rheology of kaolin suspensions*. Massachusetts Institute of Technology, PhD thesis.
- Brinkman, H. C. (1947). A calculation of the viscous force exerted by a flowing fluid on a dense swarm of particles. *Applied Scientific Research* **A1**, 27–34.
- Carrier, W. D. & Beckman, J. F. (1984). Some recent observations on the fundamental properties of remoulded clays. *Géotechnique* **34**, No. 2, 211–228.
- Gersevanov, N. M. (1934). *Dinamika mekhaniki grunkov*. (Foundation of soil mechanics.) Gosstroisdat, USSR.
- Grohse, E. W. (1955). Analysis of gas-fluidized solid

- systems by X-ray absorption. *Am. Inst. Chem. Engrs J.* **1**, No. 3, 358–365.
- Hanratty, T. J. & Bandukwala, A. (1957). Fluidization and sedimentation of spherical particles. *Am. Inst. Chem. Engrs J.* **3**, 293.
- Hawksley, P. G. W. (1951). *Some aspects of fluid flow*. London: Edward Arnold, p. 114.
- Krizek, R. J. & Somogyi, F. (1984). Perspectives on modelling consolidation of dredged materials. *Proc. ASCE Symp. on Sedimentation Consolidation Models*, San Francisco.
- Kunii, D. & Levenspiel, O. (1969). *Fluidization engineering*. New York: Wiley.
- Kynch, E. J. (1952). A theory of sedimentation. *Trans. Faraday Soc.* **48**, 168–176.
- Lewis, W. K. Gilliland, E. R. & Bauer, W. C. (1949). Characteristics of fluidized particles. *Industrial Engng Chem.* **41**, 1104–1117.
- Loeffler, A. L. & Ruth, B. F. (1959). Particulate fluidization and sedimentation of spheres. *Am. Inst. Chem. Engrs J.* **5**, 310–314.
- McRoberts, E. C. & Nixon, J. F. (1976). A theory of soil sedimentation. *Can. Geotech. J.* **13**, 294–313.
- Michaels, A. S. (1958). *Ceramic fabrication processes*, ch. 2. New York: Wiley.
- Michaels, A. S. & Bolger, J. C. (1962). Settling rates and sediment volumes of flocculated kaolin suspensions. *Industrial and Engng Chem. Fundamentals* **1**, No. 1, 24–33.
- Pane, V., Croce, P., Znidarcic, D., Ko, H.-Y., Olsen, H. W. & Schiffman, R. L. (1983). Effects of consolidation on permeability measurements for soft clay. *Géotechnique* **33**, No. 1, 67–72.
- Pane, V. (1985). *Sedimentation and consolidation of clays*. Department of Civil Engineering, University of Colorado, Boulder, PhD thesis.
- Pane, V. & Schiffman, R. L. (1985). A note on sedimentation and consolidation. *Géotechnique* **35**, No. 1, 69–72.
- Olsen, H. W. (1966). Darcy's law in saturated kaolinite. *Water Resources Research* **2**, 287–295.
- Richardson, J. F. & Zaki, W. N. (1954). Sedimentation and fluidization: Part I. *Trans. Instn Chem. Engrs* **32**, 35–53.
- Richardson, J. F. & Meikle, R. A. (1961). Sedimentation and fluidization: Part III. The sedimentation of uniform fine particles and of two-component mixture of solids. *Trans. Instn Chem. Engrs* **39**, 348–356.
- Steinour, H. (1944). Rate of sedimentation. Nonflocculated suspensions of uniform spheres. *Industrial Engng Chem.* **36**, 618–624.
- Takeda, K. (1957). Fluidization quality of fluidized bed. *Chem. Engng. (Tokyo)* **21**, No. 3, 124–129.
- Verschoor, H. (1950). Experimental data on the viscous force exerted by a flowing fluid on a dense swarm of particles. *Applied Scientific Research* **A2**, 155–161.
- Zenz, F. A. & Othmer, D. F. (1960). *Fluidization and fluid-particle systems*. New York: Reinhold.